Research Article

Pickering Emulsions of Kaffir Lime Oil Stabilized by Modified Tapioca Starch: Impact of Particle Size Reduction Methods and Octenyl Succinic Anhydride Grafting

Nuttida Kamboon and Sukanya Thepwatee*
Department of Industrial Chemistry, Faculty of Applied Science, King Mongkut's University of Technology North Bangkok, Bangkok, Thailand

Suthida Boonsith*
Department of Chemical Engineering, Faculty of Engineering, Mahidol University, Nakhon Pathom, Thailand
Expert Centre of Innovative Herbal Products (InnoHERB), Thailand Institute of Scientific and Technological Research (TISTR), Pathum Thani, Thailand

* Corresponding author. E-mail sukanya.t@sci.kmutnb.ac.th, suthida@tistr.or.th
DOI: 10.14416/j.asep.2025.08.004
Received: 16 April 2025; Revised: 14 June 2025; Accepted: 4 July 2025; Published online: 29 August 2025

Abstract
The main challenges in using tapioca starch for pickering emulsions are its native micron-sized particles, which are too large to stabilize small oil droplets, and its highly hydrophilic nature, which limits its ability to balance oil-water interfaces. This study explores the modification of tapioca starch to encapsulate kaffir lime oil (KO) in pickering emulsions, emphasizing particle size reduction and surface functionalization. Methods included enzymatic hydrolysis (alpha-amylase, alpha-amylase with glucoamylase, and pullulanase), sulfuric acid hydrolysis, and ethanol precipitation. Ethanol precipitation emerged as the most effective, producing ultra-fine particles (96–150 nm) with superior emulsion stability. Surface analysis revealed that enzymatic treatments affected particle morphology, while ethanol precipitation formed the smallest, smoothest particles and the lowest crystallinity (8.4%), compared to sulfuric acid hydrolysis, which showed the highest crystallinity (37.7%). Surface functionalization with octenyl succinic anhydride (OSA) enhanced starch hydrophobicity, confirmed by Fourier-transform infrared (FT-IR) spectroscopy and increased water contact angles. Pickering emulsions prepared with ethanol-precipitated starch esterified with 5% OSA showed the highest stability. Incorporating medium-chain triglyceride (MCT) oil at a KO/MCT ratio of 0.4/0.8 further improved droplet size and emulsion stability. These findings highlight ethanol-precipitated and OSA-modified tapioca starch as an effective bio-surfactant for stabilizing Pickering emulsions, with potential for sustainable and high-value industrial applications.

Keywords: Acid hydrolysis, Anti-solvent precipitation, Cassava starch, Enzyme hydrolysis, Octenyl succinic anhydride

1 Introduction

The modification of starch properties through particle size reduction has gained significant attention in recent years, especially for applications in emulsion stabilization [1]–[4]. Starches derived from various botanical sources–such as corn, potato, wheat, and rice–exhibit distinct physicochemical characteristics that influence their suitability for industrial use. For instance, potato starch contains large granules (2.7–70.7 μm) [5] with high swelling power and viscosity [6], while corn starch is widely used in food and pharmaceutical industries due to its high availability. Wheat starch features a bimodal granule size distribution and often contains gluten, limiting its use in allergen-free formulations [5]. Rice starch, characterized by its small granule size (<10 μm) [5], is well suited for cosmetic applications but typically exhibits limited functional stability without modification [7]. Importantly, many of these starches

contain residual lipids and proteins that may limit chemical modification processes or compromise emulsion stability [8]. In contrast, tapioca starch–derived from cassava–contains low content of lipids and proteins, which facilitates both chemical and enzymatic modifications [9]. It offers several advantages, including consistent quality, odorless and tasteless character, high purity, and low allergenicity, making it highly suitable for use in food, pharmaceutical, and cosmetic applications [10]. Tapioca starch also possesses moderate granule sizes (3–30 μm) [11], a predominantly spherical shape, and a semi-crystalline structure. Its ease of hydrolysis further enhances its applications in functional materials, especially in Pickering emulsions. These properties, combined with its renewable origin and economic viability, make tapioca starch a highly promissing candidate for scalable industrial applications.

Tapioca starch features a semi-crystalline structure consisting of two primary components: amylose, a linear poly-α-1,4-D-glucan with an amorphous structure, and amylopectin, a branched poly-α-1,4-D-glucan with α-1,6-D-glucan linkages in a crystalline structure [11]. The soft texture and hydrophilic nature of native tapioca starch are attributed to the hydroxyl groups on its glucose units.

Traditionally, tapioca starch was used in its native form without modification. However, recent research has focused on modifying starch for various industrial applications, including hydrolysis [4], [12]–[16], cross-linking [17], [18], roll/ball-milling [19], [20], and surface modification to adjust its hydrophilicity [9]. These advancements have expanded its use, particularly in Pickering emulsions, which employ solid particles to stabilize oil-water interfaces by balancing hydrophilicity and hydrophobicity, unlike conventional emulsions that rely on surfactants.

The use of starch particles in Pickering emulsions has attracted attention due to starch's biocompatibility, biodegradability, natural origin, and renewability. Tapioca starch shows promise in food [4], [21], pharmaceutical [18], and cosmetic applications [22]. However, its native micron-sized particles can be too large to efficiently stabilize small oil droplets, necessitating particle size reduction before use in Pickering emulsions.

Various methods have been explored for producing submicron starch particles, including enzymatic hydrolysis, acid hydrolysis, and anti-solvent precipitation. Acid hydrolysis improves starch crystallinity by selectively digesting amylose, leaving highly ordered amylopectin. Chen *et al*., [14] reported particle sizes similar to the original granules, while Costa *et al*., [15] achieved nanocrystalline particles (<200 nm) using acid hydrolysis. Enzymatic hydrolysis, depending on the enzyme type, can result in specific or random particle size reduction. For example, α-amylase cleaves α-1,4-glycosidic bonds, while glucoamylase cleaves both α-1,4- and α-1,6-glycosidic bonds. Pullulanase specifically targets α-1,6-glycosidic bonds, resulting in debranching [16], [23]. Ge *et al*., [24] achieved particle sizes below 200 nm through anti-solvent precipitation. Beyond size reduction, surface modification to adjust hydrophilicity/hydrophobicity, such as esterification with octenyl succinic anhydride (OSA), has gained attention for improving the stability of Pickering emulsions [25], [26]. Although numerous modification strategies have been applied to tapioca starch, comparisons across studies remain challenging due to variations in processing conditions, application types, and emulsion systems. Thus, there is significant value in modifying tapioca starch using different techniques within a single study and applying the resulting materials to the same emulsion system to evaluate their comparative performance in stabilizing Pickering emulsions.

Essential oils are widely utilized across various industries due to their diverse biological activities, including antimicrobial properties, antioxidant effects, insect repellence, and applications in aromatherapy and cosmetics [27]–[29]. However, their low water solubility, high volatility, and susceptibility to degradation pose significant limitations to their industrial applications [29], [30]. Encapsulation has emerged as a promising strategy to enhance the usability of essential oils, extend their shelf life, and preserve their bioactivity. Pickering emulsions, which rely on solid particles rather than conventional surfactants to stabilize oil-water interfaces, have gained considerable attention for essential oil encapsulation. They offer improved biocompatibility and bioactive stability, making them particularly appealing for pharmaceutical and cosmetic applications [31]–[33]. Kaffir lime essential oil, a popular ingredient in traditional medicine and cosmetics, poses specific challenges in Pickering emulsion formulation. Its low molecular weight and density (e.g., 0.8863 ± 0.002 g/cm³; [34]) contribute to a high rate of diffusion and phase separation, leading to reduced emulsion stability. Consequently, investigating strategies to enhance the stability of kaffir lime essential oil in Pickering emulsions represents an important area of research.

Accordingly, this study investigates the effect of various particle size reduction techniques, OSA surface modification on the physicochemical properties of tapioca starch and their subsequent influence on the Pickering emulsification of kaffir lime essential oil with MCT oil incorporation at different ratios on the performance of tapioca starch-stabilized Pickering emulsions containing kaffir lime essential oil—a low-density oil that poses unique formulation challenges. By systematically comparing native and modified tapioca starches, the study aims to identify the most effective modification method for essential oil encapsulation. Furthermore, the roles of OSA-modified starch and medium-chain triglycerides in enhancing emulsion stability are evaluated. The findings offer valuable insights for potential applications in food preservation, skincare, and aromatherapy formulations.

2 Materials and Methods

2.1 *Materials*

Tapioca starch was obtained from Charoenworrakit Co., Ltd. (Thailand). Glucoamylase (42,000 iu/mL) and pullulanase (400 iu/mL) were procured from Reach Biotechnology Co., Ltd. (Thailand). Alpha-amylase (320 iu/g) was procured from HiMedia Laboratories Pvt. Ltd. (India). Sulfuric acid, ethanol, and octenyl succinic anhydride (OSA) were procured from Tokyo Chemical Industry Co., Ltd. (Japan). Hydrochloric acid was procured from RCI Labscan Co., Ltd. (Thailand). Acetic acid and iso-propanol were purchased from Quality Reagent Chemical Co., Ltd. (New Zealand). Sodium acetate was purchased from Honeywell Co., Ltd. (Germany). All other chemicals were obtained from Sigma-Aldrich Chemical Co., Ltd. (USA) or Merck Co., Ltd. (Germany). Kaffir lime oil (food grade) was purchased from AP Operations Co., Ltd. (Thailand), and Myritol 318 was purchased from Chemipan Corporation Co., Ltd. (Thailand). Sudan III was obtained from Sigma-Aldrich Chemical Co., Ltd. (USA). All chemicals used in the study were of analytical grade, unless otherwise indicated.

2.2 *Preparation of enzyme pretreatment starch*

2.2.1 Alpha-amylase with/without glucoamylase

A suspension of 50.0 g of tapioca starch was prepared in 100 mL of sodium acetate buffer solution (pH 4.5) and stirred thoroughly on a hotplate stirrer at 300 rpm and 45 °C. Subsequently, 0.16 g of α-amylase (320 IU/g) and 210 µL of glucoamylase (42,000 IU/mL) were added, and the mixture was stirred continuously for 24 h. The reaction was terminated by adding 2 M HCl until the pH of the starch solution reached approximately 1.5–1.6. The suspension was stirred for an additional 30 min, after which the starch precipitate was collected by filtration and washed with deionized water until the filtrate reached a pH of approximately 6. The precipitate was then dried in an oven at 40 °C for 24 h [14]. The resulting starches were designated as “NS-Amyl” and “NS-AmylGlu.”

2.2.2 Pullulanase

A dispersion of 20.0 g of tapioca starch in 400 mL of acetic acid–sodium acetate buffer solution (pH 5.5) was prepared and heated to boiling under stirring at 300 rpm for 30 min to ensure complete gelatinization. The gelatinized starch was then cooled to 55 °C, followed by the addition of 133 µL of pullulanase (400 IU/mL). The reaction was carried out at 55 °C under continuous stirring (300 rpm) for 24 h. Enzyme activity was terminated by boiling the dispersion for 5 min. The starch precipitate was separated by centrifugation at 4500 rpm for 10 min. The collected precipitate was dried in an oven at 40 °C for 24 h, while the supernatant was freeze-dried to obtain the solid fraction. Freeze-drying was conducted after pre-freezing for up to 2 days, followed by lyophilization at –84 °C under vacuum with defrost cycles every 3 days [35]. The starch obtained from the supernatant was designated as “NS-Pull(S),” whereas the starch obtained from the precipitate was designated as “NS-Pull(P).”

2.3 *Preparation of acid hydrolysis starch*

Tapioca starch (50.0 g) was dissolved in 250 mL of 3.16 M concentrated sulfuric acid and stirred at 400 rpm at 40 °C for either 3 or 5 days. The reaction mixture was then centrifuged at 5000 rpm for 3 min, and the precipitate was collected and washed repeatedly with deionized water, with centrifugation after each wash, until the supernatant reached a pH of 6.5. The precipitate was subsequently dried at 40 °C for 24 h [36], ground thoroughly using a mortar, and stored in a desiccator. The resulting starches were designated as “NS-Sul(3)” for 3-day hydrolysis and “NS-Sul(5)” for 5-day hydrolysis.

2.4 *Preparation of ethanol nanoprecipitation starch*

Tapioca starch (5.0 g) was suspended in 500 mL of deionized water and stirred at 300 rpm at 100 °C for 30 min to ensure complete gelatinization. The mixture was then cooled to room temperature, after which 100 mL of ethanol was added dropwise at a rate of 5 mL/min under continuous stirring at 300 rpm for 8 h. The resulting starch dispersion was subsequently freeze-dried to obtain starch nanoparticles [37]. The product was designated as "NS-EtOH.".

2.5 *OSA-modification of NS-EtOH*

5.0 g of NS-EtOH was mixed with 95.0 mL of DI water at 35 °C under stirring at 300 rpm. The pH of the suspension was then adjusted to around pH 8 by adding a 3%w/v NaOH solution using a pH meter. After that, OSA was added, and the reaction was carried out for 3 h. The pH was adjusted to 6.5 using a 0.5 M HCl solution. The mixture was then centrifuged at 5,000 rpm for 3 min, followed by washing three times with ethanol and oven-dried at 40 °C for 24 h [38]. The resulting starch is referred to as "NS-EtOH-OSA". The weight percent of OSA over the dry weight of NS-EtOH is represented by the number after OSA. For example, NS-EtOH-OSA with 5% of OSA will be noted as NS-EtOH-OSA5.

2.6 *Preparation of Pickering emulsions*

Oil-in-water (O/W) Pickering emulsions were prepared by mixing 1.0 g of a starch sample with 97.8 mL of DI water under stirring at 200 rpm at 35 °C for 10 min. Subsequently, the mixture was homogenized at 15,000 rpm using a high-speed homogenizer (IKA-Werke GmbH & Co. KG) while adding a total weight of 1.2 g of the oil phase dropwise. After completing the addition of the oil phase, homogenization was continued for 3 min. Then, the resultant Pickering emulsion was stored in a glass vial at room temperature [35]. The oil phase utilized in this study consisted of Myritol 318 and kaffir lime oil, either individually or in combination.

2.7 *Characterization of starch*

2.7.1 Morphology

The surface and morphology of starch samples were observed using a scanning electron microscope (SEM, JSM-IT500LA, JEOL, Tokyo, Japan) and a field emission scanning electron microscope (FE-SEM, JSM-7610FPLUS, JEOL, Tokyo, Japan). The starch samples were placed on a sample stub using carbon tape. Subsequently, the stub and sample were coated with platinum using an auto-fine coater (JEOL Ltd. JEC-3000FC, Tokyo, Japan) [37], [39]. The morphologies were photographed at magnifications of 500× and 3,000× for SEM, while FE-SEM utilized magnifications of 3,000×and 30,000×.

Particle size measurements were performed using ImageJ software. The images were converted to 8-bit grayscale, and contrast was adjusted to enhance particle boundaries. The scale was calibrated using the "Set Scale" function, and particle size was calculated from the measured area using the "Analyze Particles" tool. The equivalent circular diameter was obtained for each particle. Multiple image regions were analyzed, and results are reported as mean ± standard deviation.

2.7.2 Fourier transform infrared (FT-IR) spectroscopy

The functional groups in native and modified starches were analyzed using a PerkinElmer Spectrum 100 FT-IR Spectrometer (PerkinElmer, Waltham, MA, USA). Samples were prepared by grinding the finely powdered starch with KBr at a ratio of 1:100. The spectra were recorded over a range of 400 to 4000 cm^{-1} with a resolution of 4 cm^{-1} and an accumulation of 9 scans [40].

2.7.3 Raman spectroscopy

Raman spectroscopy was performed at room temperature using a XploRA PLUS Confocal Raman Microscope (HORIBA Scientific, Kyoto, Japan) with an excitation wavelength of 785 nm, a slit width of 100 µm, an acquisition time of 30 s, and 3 scans [41]. Raman spectra were analyzed using LabSpec 6 software.

2.7.4 Thermal analysis

Differential scanning calorimetry (DSC) and thermogravimetric-differential thermal analysis (TGA-DTA) were employed to assess the changes in the physicochemical properties of native and modified starches. DSC analysis was carried out using a Perkin Elmer DSC 7 (Perkin Elmer, Norwalk, CT, USA). A dried starch sample (average moisture content of 7.7%) was suspended in DI water at a concentration of

30%wt and placed in a 60 µL stainless pan with a large volatile pan cover (CODE03190029) and Tygon O-rings. The total volume of the mixture was 35.9 µL. The pan was then sealed and incubated at room temperature overnight prior to the analysis. The analysis was conducted from 0°C to 120 °C with a heating rate of 10 °C/min. The onset (To), peak (Tp) and conclusion (Tc) temperatures and the melting enthalpy (ΔH) of dry samples were measured. For TGA-DTA analysis, approximately 2–3 mg of the sample was heated from 30 °C to 600 °C at a rate of 10 °C/min under a nitrogen flow of 50 mL/min, using a TGA 4000 instrument (Perkin Elmer, Waltham, MA, USA) [42], [43]. Three replicate experiments were performed.

2.7.5 Contact angle

The NS-EtOH and OSA-modified NS-EtOH samples (approximately 0.2 g each) were pressed into circular pellets with a diameter of 1.5 cm using a press machine applying a pressure of 20 MPa. An optical contact angle measurement instrument, OCA15 plus6X Parfocal zoom lens (Data Physics Instruments GmbH, Filderstadt, Germany), was utilized to measure the contact angle of the samples, with DI water serving as the test solution. During each measurement, 4 µL of liquid from a microsyringe was dispensed onto the surface of the samples at a rate of 0.5 µL/s, and the corresponding contact angle values were recorded. Three replicate experiments were performed [44].

2.7.6 X-ray diffraction

The crystal structure of starch samples was analyzed using a D2 PHASER X-ray powder diffractometer (Bruker, Germany) with Cu-Kα radiation, generated at 10 mA and 30 kV. Samples were analyzed over the range of 2θ from 10° to 40°, with a scanning rate of 1°/min and a step size of 0.02°. The particle size was determined using the Scherrer Equation (1):

$$d = k\lambda / \omega cos\theta \quad (1)$$

where d is the particle size, k is a constant close to unity, λ is the wavelength of the radiation, ω is the width on a 2θ scale, and θ is the angle of the considered Bragg reflection [45]. The crystallinity was estimated using the following equation [42]:

$$Crystallinity = (Area\ under\ the\ peaks) \times 100 / (Total\ curve\ area) \quad (2)$$

2.7.7 Degree of substation of OSA

The degree of substitution (DS) represents the average number of hydroxyl groups substituted per glucose unit. The DS of OSA-modified starches was determined by titration [25]. To perform this, 5.0 g of the OSA-modified starch sample was dispersed by stirring at 300 rpm for 30 min at room temperature in 25.0 mL of 2.5 M HCl in isopropyl alcohol solution. Following this, 100 mL of 90%v/v aqueous isopropyl alcohol solution was added, and the slurry was stirred for an additional 10 min. The solid was then filtered and washed with DI water, followed by 90%v/v aqueous isopropyl alcohol solution. Subsequently, the solid was dried in an oven at 105 °C for 3 h. Next, 1.0 g of the dried solid was mixed with 100.0 mL of DI water and heated until a clear solution was achieved. This solution was then titrated with 0.1 M NaOH. The DS was calculated using the following Equation (3):

$$DS = [0.162 \times (A \times M)/W]/[1-(0.210 \times (A \times M)/W] \quad (3)$$

where A represents the volume (in mL) of NaOH used for sample titration, W is the weight of starch (in grams), and M is the molarity of NaOH [38], [46]. Three replicate experiments were performed.

2.8 *Evaluation of Pickering emulsion*

2.8.1 Phase separation

To assess the stability of the prepared Pickering emulsions, phase separation was monitored under ambient conditions (~35 °C) for a period of up to 5 days. Photographs of the samples were captured under room light conditions.

2.8.2 Fluorescence and light microscopy

The Pickering emulsion was stained with lipophilic fluorescent dyes (Sudan III). The stained Pickering emulsion was dropped onto a glass slide, and the analysis was performed using a Leica LMD 7 fluorescence microscope (Leica, Germany). Both bright field and fluorescence modes were utilized to capture pictures of the Pickering emulsion [47].

2.8.3 Particle size distribution

The Pickering emulsion was freshly prepared prior to particle size analysis using a laser diffraction particle size analyzer (Horiba Partica mini LA-350, Japan). The emulsion sample was gradually added to the sample chamber until the transmittance reached approximately 80–90%. The analysis was repeated three times to ensure consistent results [48].

2.8.4 Zeta potential

Zeta potential was measured to assess droplet surface charge and emulsion stability. Samples were diluted 1:100 with deionized water to minimize light scattering and ionic interference, then gently shaken for uniform dispersion. Measurements were conducted at 25 ± 0.1 °C using a Zetasizer Nano ZS (Malvern Instruments, UK) with capillary cells (DTS1070) based on laser Doppler electrophoresis. Each sample was analyzed in triplicate, and average values were reported.

2.9 ***Statistical analysis***

All analyses were performed in triplicate. Statistical analysis was conducted using IBM SPSS Statistics version 28.0. One-way analysis of variance (ANOVA) followed by Tukey's post hoc test was employed to evaluate differences among sample groups. Statistically significant differences were determined at p-value < 0.05, and are indicated by different superscript letters (a, b, c, etc.) in the data presentation.

3 Results and Discussion

3.1 Appearance, texture, and morphology of treated tapioca starch

The native tapioca starch (NS) appears as a white powder with a soft, smooth texture, as confirmed by SEM images, which reveal smooth particle surfaces. After enzymatic hydrolysis treatments, both NS-Amyl and NS-AmylGlu retained properties similar to the original NS. These samples continued to exhibit a white powder form with a soft, smooth texture. The particles maintained their spherical and elliptical shapes, with smooth surfaces and diameters ranging from 11–21 µm, as indicated in Table 1 and Figure 1, consistent with reported literature [49].

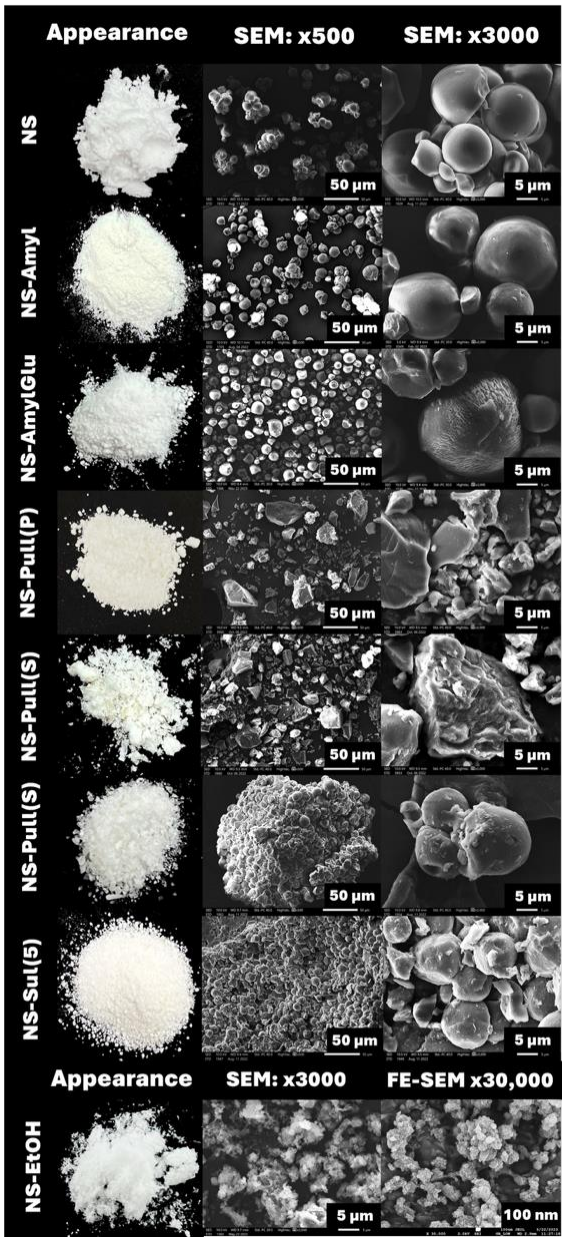

Figure 1: Appearance (left), SEM and FE-SEM images of NS, NS-Amyl, NS-AmylGlu, NS-Pull(P), NS-Pull(S), NS-Sul(3), NS-Sul(5), and NS-EtOH.

In general, α-amylase cleaves internal α-1,4-glycosidic bonds, resulting in the formation of shorter amylose chains and a reduction in the molecular weight of starch molecules. Glucoamylase hydrolyzes both α-1,4- and α-1,6-glycosidic linkages, leading to a more extensive breakdown of amylose and partial debranching of amylopectin. Pullulanase, on the other

hand, specifically targets α-1,6-glycosidic bonds, effectively debranching amylopectin and altering the native branched architecture of the starch [16], [23].

Table 1: Appearance, texture, and particle size of native and modified tapioca starches.

Sample	Appearance	Texture	Particle size (μm)
NS	White powder	Soft & Smooth	11 – 21
NS-Amyl	White powder	Soft & Smooth	15 – 20
NS-AmylGlu	White powder	Soft & Smooth	12 – 17
NS-Pull(P)	White powder	Rough	7 – 25
NS-Pull(S)	Off-white powder	Rough & Sticky	3 – 18
NS-Sul(3)	White glossy crystal	Rough & Hard	9 – 19
NS-Sul(5)	White crystal	Rough & Hard	10 – 21
NS-EtOH	White flakes	Soft & Light	0.096 – 0.150

*Particle sizes were estimated from SEM and FE-SEM images using ImageJ software.

Among the enzymatically hydrolyzed samples, only NS-Pull exhibited significant structural changes. The action of pullulanase disrupted the branched structure of amylopectin, producing linear, low-molecular weight starch fragments [16]. During freeze-drying, these fragments formed NS-Pull(S) particles, with diameters ranging from 3–18 μm, while NS-Pull(P) consisted of residual solid fractions with particle sizes of 7–25 μm. Both NS-Pull(S) and NS-Pull(P) displayed irregular, rock-like morphologies, likely due to the aggregation of molten debranched starch [50]. NS-Pull(P) retained a white powder appearance but exhibited increased surface roughness, whereas NS-Pull(S) exhibited a darker white color and a rough, sticky texture, indicating substantial internal and surface restructuring due to enzymatic debraching.

NS-Sul(3) and NS-Sul(5), on the other hand, exhibited distinct visual and structural differences. NS-Sul(3) presented a glossier, transparent, crystal-like appearance, while NS-Sul(5) appeared more opaque with a white color. Both samples had rough and hard textures. SEM images revealed that the particle morphology of NS-Sul(3) and NS-Sul(5) was somewhat similar to the original NS, displaying spherical shapes with diameters ranging from 9–19 μm for NS-Sul(3) and 10–21 μm for NS-Sul(5). However, these samples formed larger particle aggregates with rougher surfaces compared to the native starch. Sulfuric acid hydrolysis selectively degraded the amorphous regions of the starch, leaving behind the crystalline structures, which may make morphological changes less apparent in the SEM images [51].

Lastly, NS-EtOH appeared as white flakes with a soft and lightweight texture. These particles were formed after the starch was fully gelatinized and subsequently reprecipitated using ethanol. The precipitation process induced changes in the starch morphology, as the growth behavior of polymeric crystals is influenced by the chemical nature and polarity of the solvent. These factors affect the nucleation and growth of crystals, ultimately determining the resulting morphology [51]. Due to its submicron particle size, field emission scanning electron microscopy (FE-SEM) analysis was required to observe its morphology. As shown in Figure 1, NS-EtOH possessed the smallest particle size (96–150 nm) among all the hydrolyzed NS samples examined in this study. This change in morphology is consistent with the characteristics of tapioca [52], sago [53], and potato [54] starch particles obtained through the antisolvent precipitation method, as reported in the literature.

3.2 *Crystalline structure and functional group analysis*

XRD analysis is commonly employed to assess the long-range order within material structures. The results, depicted in Figure 2(a), indicate that the crystal structures and crystallinity levels of NS, NS-Amyl, NS-AmylGlu, NS-Pull(P), NS-Sul(3), and NS-Sul(5) were largely comparable. Prominent diffraction peaks were observed at scattering angles (2θ) of 15°, 17°, 18°, and 23°, characteristic of the A-type (orthorhombic) crystal structure of starch [13], [42], [55], [56]. The crystallinity values, calculated using Equation (2), were 21.5%, 21.6%, 23.3%, 22.2%, 25.0%, and 37.7%, respectively. These findings suggest that enzymatic hydrolysis using amylase, a combination of amylase and glucoamylase, or pullulanase (precipitate fraction) induced minimal alterations to the crystal structure of starch, likely due to the mild and gradual action of these enzymes under the applied conditions [57]. In contrast, sulfuric acid hydrolysis—being a strong acid treatment—selectively degraded the amorphous regions of the starch, which are more susceptible to hydrolysis, thereby enriching the crystalline fraction [58].

Extending the hydrolysis time from three to five hours further increased the relative crystallinity, highlighting the critical role of treatment duration in determining the extent of hydrolysis. These results are consistent with previous reports [13], [59].

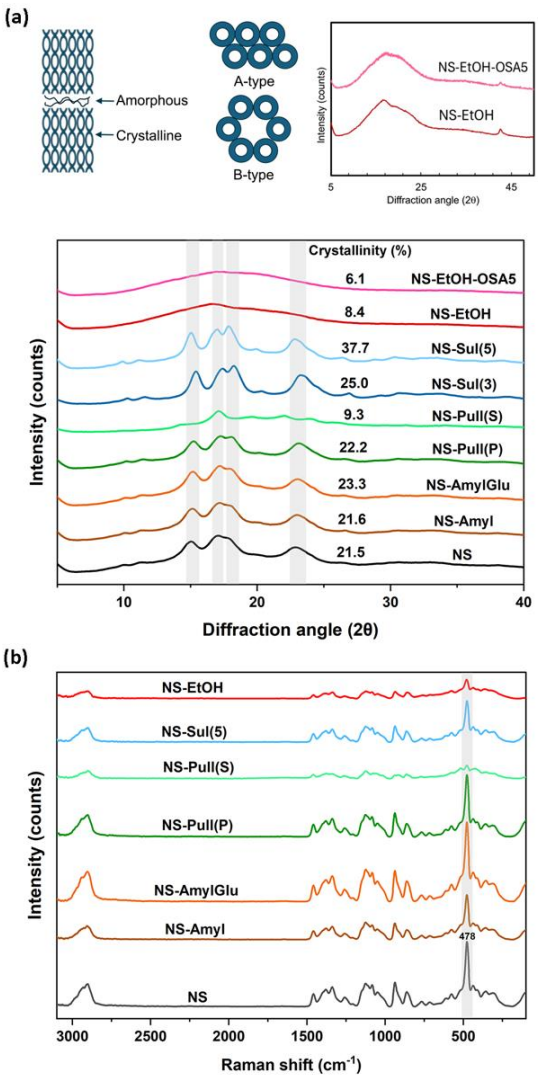

Figure 2: (a) XRD diffractograms and (b) Raman spectra of native and treated tapioca starches.

In contrast, NS-Pull(S) displayed diffraction peaks at 2θ values of 17°, 22°, and 24°, with a crystallinity of 9.3%, indicative of a B-type (hexagonal) crystal structure [13], [42], [55], [56]. This suggests the formation of a new crystalline phase from glucan chains during the freeze-drying process, albeit with reduced crystallinity. The supernatant fraction of NS hydrolyzed by pullulanase (NS-Pull(S)) underwent substantial changes in its crystalline structure, marked by a change in diffraction peaks and a significant reduction in crystallinity. These structural modifications are attributed to the recrystallization of newly formed particles, consisting of linear glucan chains produced by pullulanase hydrolysis.

NS-EtOH, obtained via ethanol precipitation, exhibited no distinct diffraction peaks and displayed the lowest crystallinity, at 8.4%, indicative of a predominantly amorphous structure. Ethanol precipitation appears to have almost completely transformed the crystalline structure of NS into an amorphous form, likely due to recrystallization effects during the precipitation and drying processes. Despite the similar crystallinity levels of NS-Pull(S) and NS-EtOH, the particle sizes observed through SEM and FE-SEM were significantly larger for NS-Pull(S).

Raman spectroscopy was employed to investigate the functional groups and short-range order present in both NS and the treated NS samples. Starch is comprised of amylose and amylopectin, both of which consist of glucose monomers linked by α-1,4 glycosidic bonds (present in both amylose and amylopectin) and α-1,6 glycosidic bonds (found exclusively in amylopectin). As shown in Figure 2(b), the peak observed at 478 cm^{-1} corresponds to the υ(C–C–O) and δ(C–C–O) of the pyranose ring skeletal [60]. The Raman signal around 880 cm^{-1} is attributed to the stretching of the ring υ_s(C–O–C), as well as δ(C–H, CH_2) modes. Similarly, the signal at 930 cm^{-1} in the starch spectrum is typically associated with the υ_s(C–O–C) vibrations of α-1,4 glycosidic bonds [61]. The peak at 1083 cm^{-1} is indicative of δ(C–OH) vibration, while the signal at 1127 cm^{-1} corresponds to υ(C–OH), δ(C–OH), and υ(C–O) vibration modes. The signal at 1262 cm^{-1} represents $\delta(CH_2)$ and C–OH/ CH_2OH (side chain) vibrations, and the peak at 1341 cm^{-1} corresponds to $\delta(CH_2)$, twisting and δ(C–OH) vibrations. The signal at 1382 cm^{-1} is associated with δ(C–OH), δ(C–H) bending, and δ(CH_2) scissoring, while the signal at 1461 cm^{-1} suggests the $\delta_s(CH_2)$ twisting and C–H bending [61]. Finally, the signal at 2900 cm^{-1} corresponds to the υ(C–H) stretching vibrations in aliphatic hydrocarbons. These findings are consistent with the XRD results, which demonstrated a decrease in long-range order for NS-EtOH and NS-Pull(S).

3.3 *Thermal properties*

DSC was employed to investigate the changes in the gelatinization properties of treated starch samples compared to native starch (NS). The onset (To), peak (Tp), conclusion (Tc) temperatures, gelatinization range (Tc-To) and gelatinization enthalpy (ΔH) are summarized in Table 2. NS exhibited a broad endothermic peak (Figure 3), with To, Tp, Tc, and ΔH values of 63.51 ± 0.27 °C, 69.89 ± 0.67 °C, 80.54 ± 0.69 °C, 17.03 °C, and 15.81 ± 0.49 J/g, respectively.

Following enzymatic treatments, both NS-Amyl and NS-AmylGlu exhibited thermal properties similar to NS, with a slightly narrower gelatinization range. This suggests that hydrolysis using amylase, or a combination of amylase and glucoamylase, only slightly altered the starch granule structure, as the ΔH values reflect the thermal energy required to break down crystallites and disassemble double helices in both crystalline and non-crystalline regions [50], [62]. Although a slight decrease in the gelatinization range was observed, possibly due to more uniform short chains in amylopectin, the change was minimal, indicating that the overall structure remained largely comparable to that of native starch.

For NS-Pull(P), a slight increase in the onset temperature (To) to 68.89 ± 0.05 °C and peak temperature (Tp) to 73.33 ± 0.00 °C was observed, while the conclusion temperature (Tc) remained similar to that of NS at 79.81 ± 0.40 °C. The gelatinization range was reduced, along with a slight decrease in gelatinization enthalpy (ΔH) to 14.62 ± 0.45 J/g. These higher To and Tp values may result from more homogeneous amylopectin within the starch granule after partial hydrolysis by pullulanase. The narrower gelatinization range suggests a more uniform crystal distribution [62]. Nonetheless, as previously mentioned, the changes were minimal, indicating that the structure remains largely comparable to that of native starch.

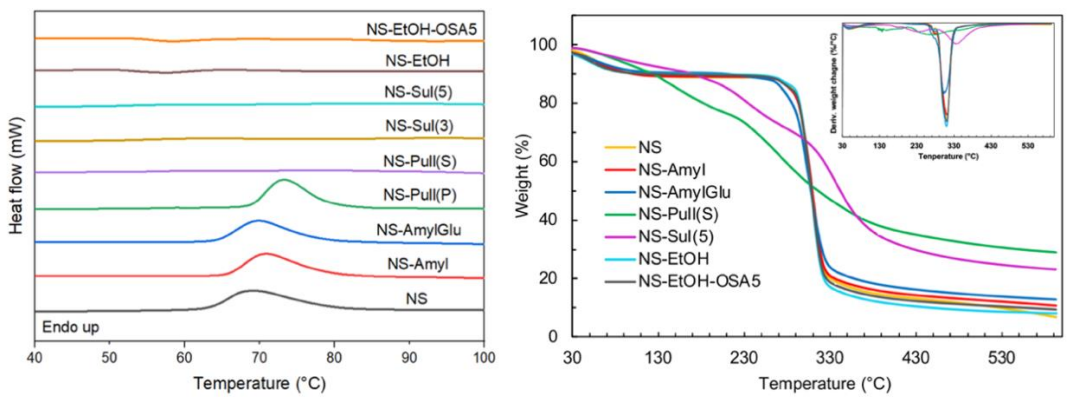

Figure 3: DSC thermograms (left) and TGA/DTG thermograms (right) of native and hydrolyzed starches.

However, NS-Pull(S), NS-Sul(3), NS-Sul(5), and NS-EtOH did not exhibit the sharply defined endothermic peaks typically associated with starch gelatinization in water. For NS-Pull(S) and NS-EtOH, this could be attributed to their more amorphous structures, which gelatinize more easily compared to native starch (NS), making detection via DSC challenging [42], [54]. Studies have observed minimal gelatinization with low enthalpy in such samples, further confirming their altered structure. Despite the higher crystallinity of NS-Sul(3) and NS-Sul(5) observed via XRD, the absence of peaks may result from the fact that gelatinization is influenced not only by crystalline order but also by the amorphous regions [63]. Acid hydrolysis predominantly targets these amorphous areas, leaving behind more ordered, crystalline structures. If hydrolysis is extensive, the remaining structure may be highly crystalline but lack the amorphous regions necessary for water absorption and swelling, both of which are critical for gelatinization.

TGA-DTG analysis was conducted to evaluate the thermal stability of the starch samples under a nitrogen atmosphere. The initial weight loss observed below 130 °C was attributed to the evaporation of absorbed water. A subsequent weight loss occurring below 300 °C was linked to the devolatilization of starch granules, while the weight loss at higher temperatures corresponded to the thermal decomposition of the starch, leaving behind residual unburnt carbon or biochar [42]. Most samples left a

solid residue of approximately 10% following thermal degradation. However, the NS-Pull(S) and NS-Sul(5) samples exhibited significantly higher residual contents, approximately 28% and 23%, respectively. Jiang *et al*., [64] found that grafting OSA weakened the internal hydrogen bonding of starch and lowered its decomposition temperature. However, in our study, when comparing NS-EtOH and NS-EtOH-OSA5, we observed no significant shift in the decomposition temperature. This could be attributed to the amorphous structure of NS-EtOH, which may have limited the impact of OSA grafting on the decomposition behavior.

Table 2: Differential thermal properties of native, hydrolyzed, and OSA-modified starches.

Sample	To (°C)	Tp (°C)	Tc (°C)	Tc-To (°C)	Enthalpy (ΔH, J/g)
NS	63.51 ± 0.27 [a]	69.89 ± 0.67[a]	80.54 ± 0.69[a]	17.03	15.81 ± 0.49[a]
NS-Amyl	65.87 ± 0.02[b]	70.67 ± 0.17[b]	79.33 ± 0.19[a]	13.46	15.16 ± 0.41[a]
NS-AmylGlu	63.79 ± 0.16[a]	69.83 ± 0.00[a]	78.34 ± 0.08[a]	14.55	14.89 ± 0.26[a]
NS-Pull(P)	68.89 ± 0.05[c]	73.33 ± 0.00[c]	79.81 ± 0.40[a]	10.92	14.62 ± 0.45[a]
NS-Pull(S)	ND	ND	ND	ND	ND
NS-Sul(3)	ND	ND	ND	ND	ND
NS-Sul(5)	ND	ND	ND	ND	ND
NS-EtOH	ND	ND	ND	ND	ND
NS-EtOH-OSA5	ND	ND	ND	ND	ND

ND = not detected

3.4 *Screening of treated NS for Pickering emulsion of kaffir lime oil*

To assess the potential of treated NS samples and identify the most suitable treatment for Pickering emulsion formation, emulsions were prepared using kaffir lime oil (KO) as the oil phase. Figure 4 illustrates the freshly prepared emulsions and their stability after one day of storage under ambient conditions (~35 °C). Among the various treatments (NS-Amyl, NS-AmylGlu, NS-Pull(P), NS-Pull(S), NS-Sul(3), NS-Sul(5)), NS-EtOH exhibited the highest stability. This superior stability is likely attributed to the smaller particle size of NS-EtOH compared to the other treated NS samples. The stability of Pickering emulsions is influenced by several factors, including particle size, the hydrophilic/hydrophobic balance, and the surface charge of the solid particles. These particles adsorb at the oil–water interface, forming a mechanical barrier that prevents droplet coalescence through steric hindrance. Among these parameters, particle size is particularly critical; for effective stabilization, the particles must be significantly smaller than the emulsion droplets. Smaller particles can more efficiently pack at the interface, forming a dense layer that enhances emulsion stability and prevents droplet aggregation [2], [65]. Based on these findings, NS-EtOH was selected for OSA modification and further investigation as a stabilizer in KO-based Pickering emulsions.

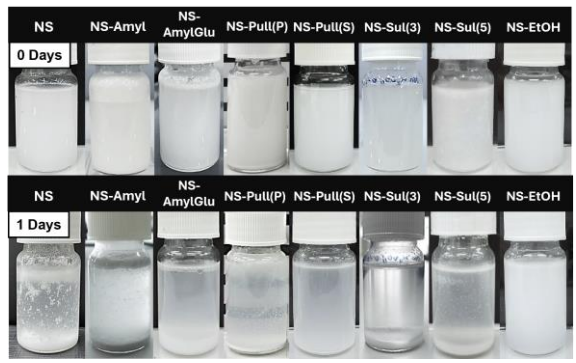

Figure 4: Pickering emulsions of KO prepared with native and hydrolyzed starches, shown both immediately after preparation and following one day of storage at room temperature.

3.5 OSA modification of NS-EtOH

3.5.1 Functional group analysis using FT-IR

NS-EtOH was modified with OSA through an esterification reaction, using various concentrations ranging from 1% to 7% (w/w). The successful grafting of OSA onto the NS-EtOH particles was confirmed via FT-IR spectroscopy. Additionally, the degree of substitution (DS) and contact angle of the modified NS-EtOH-OSA samples were measured to assess their potential for stabilizing Pickering emulsions.

Figure 5 displays the FT-IR spectra of both NS-EtOH and NS-EtOH-OSA samples. As starch is composed of glucose units linked by glycosidic bonds, it was expected that the FT-IR spectrum of NS-EtOH would show characteristic vibrational peaks corresponding to O–H, C–H, and C–O bonds. As anticipated, NS-EtOH exhibited peaks at 3390 cm^{-1} (O–H stretching), 2928 cm^{-1} (C–H stretching), 1638 cm^{-1} (H–O–H bending, from absorbed water), 1155 cm^{-1} (C–O stretching, C–O–C), 1080 cm^{-1} (C–O stretching), 1021 cm^{-1} (C–O stretching), and 930 cm^{-1} (C–O stretching) [42], [43].

Since NS-EtOH-OSA retains the starch backbone, all modified samples displayed peaks at 3390 cm^{-1} (O–H stretching), 2928 cm^{-1} (C–H stretching), 1638 cm^{-1} (O–H bending), 1155 cm^{-1} (C–O stretching, C–O–C), 1080 cm^{-1} (C–O stretching), 1021 cm^{-1} (C–OH stretching), and 930 cm^{-1} (C–O stretching) [66]. Additionally, the characteristic vibrational peaks of carboxylate ($RCOO^-$) groups from the grafted OSA were observed, including asymmetric stretching of C–O at 1572 cm^{-1} [66], [67] and stretching vibrations of C=O at 1724 cm^{-1}[43], [66]. These peaks appeared in all OSA-modified samples, from 1% to 7% (w/w), confirming the successful grafting of OSA onto the NS-EtOH particles. However, the signals were relatively weak, making it challenging to clearly distinguish them as the OSA concentration increased. Consequently, further analysis was performed to examine the degree of substitution and contact angle of the NS-EtOH-OSA samples.

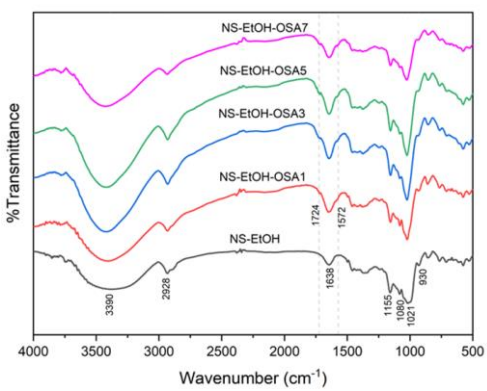

Figure 5: FT-IR spectra of NS-EtOH and NS-EtOH-OSA at OSA concentrations ranging from 1% to 7% (w/w).

3.5.2 Degree of substitution of OSA and contact angle, and Pickering emulsion of kaffir lime oil

As illustrated in Figure 6, the degree of substitution (DS) increased with the concentration of OSA used in the esterification process. The DS values were 0.008 ± 0.001, 0.014 ± 0.003, 0.018 ± 0.002, and 0.019 ± 0.001, corresponding to OSA concentrations of 1%, 3%, 5%, and 7% (w/w), respectively. These values were slightly lower than those reported in previous studies, likely due to the reaction being performed at a lower pH [68]. Simultaneously, the contact angle of NS-EtOH increased from 43.5 ± 0.3° to 48.8 ± 0.4° at 1% OSA (NS-EtOH-OSA1) and further rose to 52.9 ± 0.3° with 5% OSA (NS-EtOH-OSA5). This is in agreement with earlier findings showing that starch with OSA and a DS of 0.018 exhibits a contact angle of approximately 50° [26]. However, further increasing the OSA concentration to 7% (w/w) did not result in a significant rise in the contact angle, which aligns with the relatively modest increase in DS. The observed increases in DS and contact angle with higher OSA concentrations confirm the successful substitution of OSA onto the starch surface, corroborating the FT-IR results.

3.5.3 Pickering emulsion of kaffir lime oil using NS-EtOH-OSA

To investigate the effect of hydrophilicity/ hydrophobicity on the stability of kaffir lime oil Pickering emulsions, NS-EtOH-OSA with varying OSA concentrations (1–7% (w/w)) was used to prepare the emulsions. As shown in Figure 6, the freshly prepared emulsions appeared homogeneous and were indistinguishable. However, light microscope images revealed that increasing OSA concentrations led to a reduction in droplet size in the resulting Pickering emulsions. In addition, after two days of storage at room temperature, noticeable changes became evident. Notably, NS-EtOH-OSA5 produced the most stable Pickering emulsion, exhibiting minimal phase separation. In contrast, emulsions prepared with other OSA concentrations displayed varying degrees of phase separation, including creaming, sedimentation, or both.

Consequently, NS-EtOH-OSA5 was selected for further investigation, including XRD, DSC, and TGA/DTG analysis, to assess the impact of OSA grafting on the structure and thermal properties of the modified starch. The analysis revealed a slight alteration in the crystal structure of NS-EtOH-OSA5, with a decrease in crystallinity to 6.1% (Figure 2(a)) compared to the 8.4% observed in NS-EtOH. This suggests that OSA modification affected the internal order of the starch structure [69]. Although increasing OSA concentrations during the grafting process did induce some changes in the crystal structure, the impact was minimal. Even with the OSA concentration raised to 7% (w/w) (NS-EtOH-OSA7), the crystallinity remained relatively stable at 6.4% (data not shown). Thus, the primary crystal structure of NS-EtOH was largely preserved. The thermal properties observed through DSC (Figure 3 and Table 2) and TGA/DTG (Figure 3) analysis were similar to those of NS-EtOH.

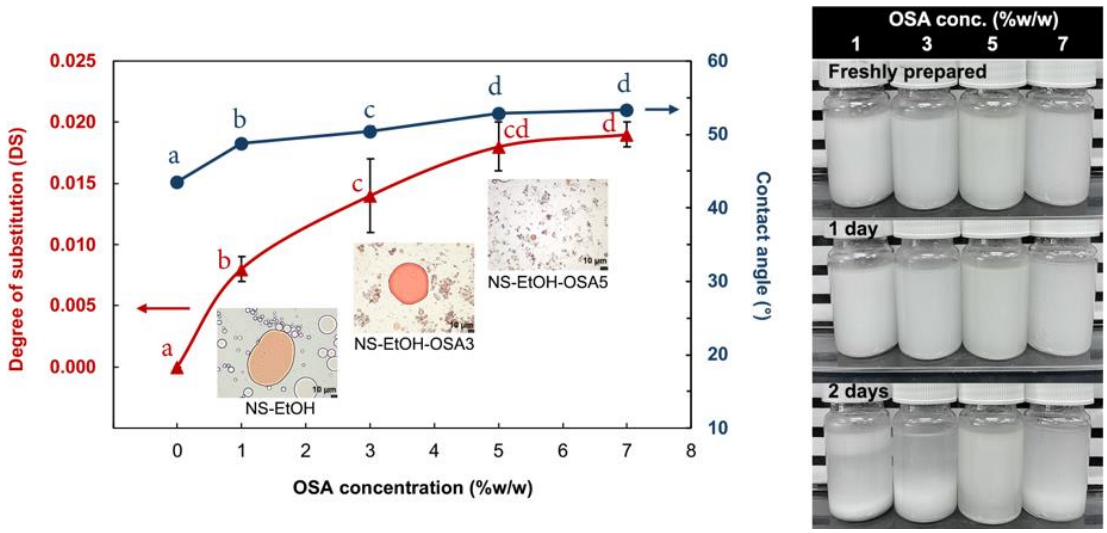

Figure 6: Degree of substitution of OSA, contact angle, and behavior of pickering emulsions for OSA-modified NS-EtOH at various OSA concentrations.

3.6 *Effect of MCT addition on Pickering emulsion droplet size and stability*

To investigate the influence of medium chain triglyceride (MCT, Myritol 318 - Caprylic/Capric Triglyceride) on kaffir lime oil Pickering emulsion behavior, MCT was blended with KO at different KO/MCT weight ratios of 0.4/0.8, 0.5/0.7, 0.6/0.6, 0.7/0.5, and 0.8/0.4, while maintaining the total oil phase constant. Figure 7 illustrates the appearance, as well as light and fluorescence microscopy images of the prepared Pickering emulsions.

The freshly prepared emulsions indicated that the addition of a small amount of MCT facilitated the formation of stable Pickering emulsions. However, as the MCT concentration increased, droplet agglomeration became more pronounced, leading to accelerated phase separation. After five days of storage at under ambient conditions (~35 °C), the emulsion with a KO/MCT ratio of 0.4/0.8 demonstrated the highest stability, with only slight sedimentation and minimal phase separation. This improved stability is likely due to a reduction in Ostwald ripening, as MCT oil–being less water-soluble than essential oil–limits the diffusion of oil molecules between droplets [36]. Moreover, MCT contributes to balancing the density between the oil and aqueous phases, thereby reducing gravitational separation [36].

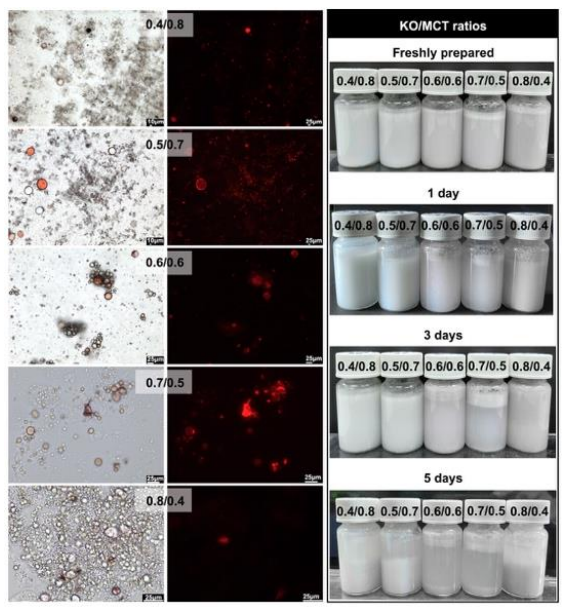

Figure 7: Light microscopy (left) and fluorescence microscopy (middle) images of freshly prepared Pickering emulsions with varying KO/MCT ratios. Photographs (right) show the formulations over a 5-day storage period to observe stability.

In contrast, emulsions with KO/MCT ratios of 0.6/0.6 and 0.7/0.5 exhibited both sedimentation and creaming, while at a KO/MCT ratio of 0.8/0.4, sedimentation became the dominant instability mechanism. Although increasing MCT content can suppress Ostwald ripening, excessively high oil

concentrations may lead to droplet coalescence if emulsifier coverage is inadequate. Additionally, factors such as emulsifier concentration and type, droplet size distribution, and interfacial properties also play critical roles in determining the overall emulsion performance.

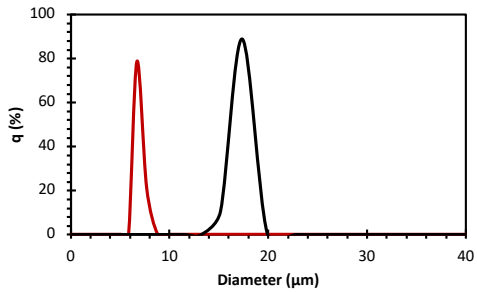

Figure 8: Droplet size distribution of Pickering emulsions prepared with pure KO (black line) and with a KO/MCT ratio of 0.4/0.8 (red line).

Light and fluorescence microscopy revealed that at a KO/MCT ratio of 0.4/0.8, the Pickering droplets were smaller and more homogeneous than those in emulsions with higher MCT content. Droplet size distribution, as shown in Figure 8, indicated that emulsions prepared with pure KO had larger droplets with a broader size distribution, as evidenced by the peak width at half height. The addition of MCT effectively reduced the droplet size, leading to enhanced stability. This confirms that MCT facilitates both the formation and stability of KO Pickering emulsions.

Table 3: Zeta potential of Pickering emulsions prepared with various KO/MCT ratios and with pure KO (1.2/0.0).

KO/MCT	Zeta Potential (mV)
0.4/0.8	-32.6 ± 0.7[a]
0.5/0.7	-30.9 ± 0.6[a]
0.6/0.6	-17.3 ± 2.9[b]
0.7/0.5	-11.8 ± 2.2[c]
0.8/0.4	-10.0 ± 1.7[c]
1.2/0.0	-11.0 ± 1.9[c]

Table 3 presents the zeta potential values of Pickering emulsions prepared with various KO/MCT ratios. Zeta potential is a key factor influencing the stability of emulsions. Typically, high absolute values of zeta potential (greater than ±30 mV), whether positive or negative, enhance emulsion stability by providing strong electrostatic repulsion between droplets [70]. This repulsion prevents droplet aggregation and delays phase separation. The results indicate that emulsions with KO/MCT ratios of 0.4/0.8 and 0.5/0.7 exhibited the highest (most negative) zeta potential values, at –32.6 ± 0.7 mV and –30.9 ± 0.6 mV, respectively. These high negative charges contributed to their superior stability compared to emulsions prepared with higher KO ratios, which showed lower zeta potential values.

4 Conclusions

This study explored the impact of various particle size reduction techniques, OSA surface modification, and MCT oil incorporation on the performance of tapioca starch-stabilized Pickering emulsions containing kaffir lime essential oil—a low-density oil that poses unique formulation challenges. The methods included enzymatic hydrolysis with alpha-amylase, a combination of alpha-amylase and glucoamylase, pullulanase, sulfuric acid hydrolysis, and ethanol precipitation. Each technique altered the starch characteristics uniquely, with ethanol precipitation yielding the smallest particles (0.096–0.150 µm) and the lowest crystallinity (8.4%). Surface modification with octenyl succinic anhydride (OSA) at a concentration ranging from 1–7% was used to improve emulsion stability. Fourier-transform infrared (FT-IR) analysis confirmed successful OSA grafting, as evidenced by new peaks at 1724 cm^{-1} and 1572 cm^{-1}, indicating effective modification. Increased degree of substitution (DS) and water contact angle further supported this modification. Among the emulsions prepared, the one utilizing ethanol-precipitated tapioca starch esterified with 5% OSA demonstrated the highest stability. Additionally, incorporating medium-chain triglyceride (MCT) oil at a KO/MCT ratio of 0.4/0.8 resulted in the smallest droplet size, highest zeta potential, and most stable Pickering emulsion.

These findings suggest that ethanol-precipitated starch with optimal OSA modification and appropriate MCT blending offers a robust approach for developing stable Pickering emulsions for encapsulating kaffir lime oil. These findings enhance our understanding of how starch structure and physicochemical properties influence emulsion behavior, offering practical guidance for improving stability of pickering emulsion using low-density oils such as essential oils. This study also highlights the potential of modified tapioca starch as a sustainable, high-performance bio-surfactant with potential applications in pharmaceuticals, food preservation, cosmetics, aromatherapy, and other related industries.

Acknowledgments

We gratefully acknowledge the research funding provided by King Mongkut's University of Technology North Bangkok (grant number: KMUTNB-67-BASIC-18) and the partial support from the National Research Council of Thailand (NRCT) (grant number: N21A650062). We also extend our gratitude to the Mahidol University-Frontier Research Facility (MU-FRF) and the Department of Chemical Engineering, Mahidol University, for their invaluable support with instrumentation. Special thanks are due to the scientists of MU-FRF for their technical expertise and assistance with FE-SEM, DLS, Raman spectroscopy, and DSC analyses. Their guidance was instrumental in the success of this project.

Author Contributions

N. K.: investigation, methodology, visualization, writing – methodology, and graphic preparation; S. B.: conceptualization, resources, supervision, validation, and project administration; S. T.: conceptualization, data curation, formal analysis, graphic preparation, writing – original draft, reviewing, and editing, funding acquisition, supervision, project administration, and validation.

Conflicts of Interest

The authors declare no conflict of interest.

References

[1] H. Lu and Y. Tian, "Nanostarch: Preparation, modification, and application in Pickering emulsions," *Journal of Agricultural and Food Chemistry*, vol. 69, pp. 6929–6942, Jun. 2021, doi: 10.1021/acs.jafc.1c01244.

[2] R. L. J. Almeida, S. S. Monteiro, N. C. Santos, N. S. Rios, and E. S. dos Santos, "Starch modification and its application in Pickering emulsion stabilization: A review," *Journal of Food Measurement and Characterization*, vol. 18, pp. 4984–5003, May 2024, doi: 10.1007/s11694-024-02550-6.

[3] C. Guida, A. C. Aguiar, and R. L. Cunha, "Green techniques for starch modification to stabilize Pickering emulsions: A current review and future perspectives," *Current Opinion in Food Science*, vol. 38, pp. 52–61, Apr. 2021, doi: 10.1016/j.cofs.2020.10.017.

[4] F. Zhu, "Starch based Pickering emulsions: Fabrication, properties, and applications," *Trends in Food Science & Technology*, vol. 85, pp. 129–137, Mar. 2019, doi: 10.1016/j.tifs.2019.01.012.

[5] L. Guo, H. Chen, Y. Zhang, S. Yan, X. Chen, and X. Gao, "Starch granules and their size distribution in wheat: Biosynthesis, physicochemical properties and their effect on flour-based food systems," *Computational and Structural Biotechnology Journal*, vol. 21, pp. 4172–4186, Aug. 2023, doi: 10.1016/j.csbj.2023.08.019.

[6] R. Jia, C. Cui, L. Gao, Y. Qin, N. Ji, L. Dai, Y. Wang, L. Xiong, R. Shi, and Q. Sun, "A review of starch swelling behavior: Its mechanism, determination methods, influencing factors, and influence on food quality," *Carbohydrate Polymers*, vol. 321, p. 121260, Aug. 2023, doi: 10.1016/j.carbpol.2023.121260.

[7] P. P. Wang, Z. G. Luo, and T. M. Tamer, "Effects of octenyl succinic anhydride groups distribution on the storage and shear stability of Pickering emulsions formulated by modified rice starch," *Carbohydrate Polymers*, vol. 228, p. 115389, Sep. 2020, doi: 10.1016/j.carbpol.2019.115389.

[8] H. W. Choi and H.-S. Kim, "Hydroxypropylation and acetylation of rice starch: Effects of starch protein content," *Food Science and Biotechnology*, vol. 31, no. 9, pp. 1169–1177, Jun. 2022, doi: 10.1007/s10068-022-01106-y.

[9] Z. Wang, P. Mhaske, A. Farahnaky, S. Kasapis, M. Majzoobi, "Cassava starch: Chemical modification and its impact on functional properties and digestibility, a review," *Food Hydrocolloids*, vol. 129, p. 107542, Jan. 2022, doi: 10.1016/j.foodhyd.2022.107542.

[10] S. Das et al., "Advances of cassava starch-based composites in novel and conventional drug delivery systems: a state-of-the-art review," *RSC Pharmaceutics*, vol. 1, no. 2, pp. 182–203, Mar. 2024, doi: 10.1039/D3PM00008G.

[11] D. Le Corre, J. Bras, and A. Dufresne, "Starch nanoparticles: A review," *Biomacromolecules*, vol. 11, pp. 1139–1153, Apr. 2010, doi: 10.1021/bm901428y.

[12] N. Atichokudom-chai, S. Shobsngob, P. Chinachoti, and S. Varavinit, "A study of some physicochemical properties of high-crystalline tapioca starch," *Starch - Stärke*, vol. 53, pp. 577–

581, Oct. 2001, doi: 10.1002/1521-379X(200111)53:11<577::AID-STAR577>3.0.CO;2-0.

[13] P. Chen, F. Xie, L. Zhao, Q. Qiao, and X. Liu, "Effect of acid hydrolysis on the multi-scale structure change of starch with different amylose content," *Food Hydrocolloids*, vol. 69, pp. 359–368, Aug. 2017, doi: 10.1016/j.foodhyd.2017.03.003.

[14] Y. Chen, S. Huang, Z. Tang, X. Chen, and Z. Zhang, "Structural changes of cassava starch granules hydrolyzed by a mixture of α-amylase and glucoamylase," *Carbohydrate Polymers*, vol. 85, pp. 272–275, Apr. 2011, doi: 10.1016/j.carbpol.2011.01.047.

[15] É.K.d.C. Costa, C.O. de Souza, J.B.A. da Silva, and J.I. Druzian, "Hydrolysis of part of cassava starch into nanocrystals leads to increased reinforcement of nanocomposite films," *Journal of Applied Polymer Science*, vol. 134, p. 45311, Jul. 2017, doi: 10.1002/app.45311.

[16] S. L. Hii, J.S. Tan, T. C. Ling, and A. B. Ariff, "Pullulanase: Role in starch hydrolysis and potential industrial applications," *Enzyme Research*, vol. 2012, p. 921362, Sep. 2012, doi: 10.1155/2012/921362.

[17] R. Wongsagonsup, T. Pujchakarn, S. Jitrakbumrung, W. Chaiwat, A. Fuongfuchat, S. Varavinit, S. Dangtip, and M. Suphantharika, "Effect of cross-linking on physicochemical properties of tapioca starch and its application in soup product, *Carbohydrate Polymers*, vol. 101, pp. 656–665, Jan. 2014, doi: 10.1016/j.carbpol.2013.09.100.

[18] N. Atichokudomchai and S. Varavinit, "Characterization and utilization of acid-modified cross-linked Tapioca starch in pharmaceutical tablets," *Carbohydrate Polymers*, vol. 53, pp. 263–270, Aug. 2003, doi: 10.1016/S0144-8617(03)00070-5.

[19] Q. Wang, L. Li, and X. Zheng, A review of milling damaged starch: "Generation, measurement, functionality and its effect on starch-based food systems," *Food Chemistry*, vol 315, pp. 126267, Jun. 2020, doi: 10.1016/j.foodchem.2020.126267.

[20] S. P. Bangar, A. Singh, A. O. Ashogbon, and H. Bobade, "Ball-milling: A sustainable and green approach for starch modification," *International Journal of Biological Macromolecules*, vol. 237, p. 124069, May 2023, doi: 10.1016/j.ijbiomac.2023.124069.

[21] X. Guo, X. Wang, Y. Wei, P. Liu, X. Deng, Y. Lei, and J. Zhang, "Preparation and properties of films loaded with cellulose nanocrystals stabilized Thymus vulgaris essential oil Pickering emulsion based on modified tapioca starch/polyvinyl alcohol," *Food Chemistry*, vol. 435, p. 137597, Mar. 2024, doi: 10.1016/j.foodchem.2023.137597.

[22] B. Pang, H. Liu, and K. Zhang, "Recent progress on Pickering emulsions stabilized by polysaccharides-based micro/nanoparticles," *Advances in Colloid and Interface Science*, vol. 296, p. 102522, Oct. 2021, doi: 10.1016/j.cis.2021.102522.

[23] H. Zhang and Z. Jin, "Preparation of resistant starch by hydrolysis of maize starch with pullulanase," *Carbohydrate Polymers*, vol. 83, pp. 865–867, Jan. 2011, doi: 10.1016/j.carbpol.2010.08.066.

[24] S. Ge, L. Xiong, M. Li, J. Liu, J. Yang, R. Chang, C. Liang, and Q. Sun, "Characterizations of Pickering emulsions stabilized by starch nanoparticles: Influence of starch variety and particle size," *Food Chemistry*, vol. 234, pp. 339–347, Nov. 2017, doi: 10.1016/j.foodchem.2017.04.150.

[25] F. Zhou, M. Dong, J. Huang, G. Lin, J. Liang, S. Deng, C. Gu, and Q. Yang, "Preparation and physico-chemical characterization of OSA-modified starches from different botanical origins and study on the properties of Pickering emulsions stabilized by these starches," *Polymers*, vol. 15, p. 706, Jan. 2023, doi: 10.3390/polym15030706.

[26] Z.-Y. Yu, S.-W. Jiang, Z. Zheng, X.-M. Cao, Z.-G. Hou, J.-J. Xu, H.-L. Wang, S.-T. Jiang, and L.-J. Pan, "Preparation and properties of OSA-modified taro starches and their application for stabilizing Pickering emulsions," *International Journal of Biological Macromolecules*, vol. 137, pp. 277–285, Sep. 2019, doi: 10.1016/j.ijbiomac.2019.06.230.

[27] A. R. Mukurumbira, R. A. Shellie, R. Keast, E.A. Palombo, and S.R. Jadhav, "Encapsulation of essential oils and their application in antimicrobial active packaging," *Food Control*, vol. 136, p. 108883, Jun. 2022, doi: 10.1016/j.foodcont.2022.108883.

[28] Y. Cahyana, Y. S .E. Putri, D. S. Solihah, F. S. Lutfi, R. M. Alqurashi, and H. Marta, "Pickering emulsions as vehicles for bioactive compounds

from essential oils," *Molecules*, vol. 27, p. 7872, Nov. 2022, doi: 10.3390/molecules27227872.

[29] H. Majeed, Y.-Y. Bian, B. Ali, A. Jamil, U. Majeed, Q. F. Khan, K. J. Iqbal, C. F. Shoemaker, and Z. Fang, "Essential oil encapsulations: Uses, procedures, and trends," *RSC Advances*, vol. 5, pp. 58449–58463, Jun. 2015, doi: 10.1039/C5RA06556A.

[30] B. Horváth, S. Pál, and A. Széchenyi, "Preparation and in vitro diffusion study of essential oil Pickering emulsions stabilized by silica nanoparticles," *Flavour and Fragrance Journal*, vol. 33, pp. 385–396, Aug. 2018, doi: 10.1002/ffj.3463.

[31] A. E. Asbahani, K. Miladi, W. Badri, M. Sala, E. H. A. Addi, H. Casabianca, A. E. Mousadik, D. Hartmann, A. Jilale, F. N. R. Renaud, and A. Elaissari, "Essential oils: From extraction to encapsulation," *International Journal of Pharmaceutics*, vol. 483, pp. 220–243, Apr. 2015, doi: 10.1016/j.ijpharm.2014.12.069.

[32] C. Burgos-Díaz, F. Leal-Calderon, Y. Mosi-Roa, M. Chacón-Fuentes, K. Garrido-Miranda, M. Opazo-Navarrete, A. Quiroz, and M. Bustamante, "Enhancing the retention and oxidative stability of volatile flavors: A novel approach utilizing O/W Pickering emulsions based on agri-food byproducts and spray-drying," *Foods*, vol. 13, p. 1326, Apr. 2024, doi:10.3390/foods13091326.

[33] Y. Cheng, X. Cai, X. Zhang, Y. Zhao, R. Song, Y. Xu, and H. Gao, "Applications in Pickering emulsions of enhancing preservation properties: Current trends and future prospects in active food packaging coatings and films," *Trends in Food Science and Technology*, vol. 151, p. 104643, Sep. 2024, doi: 10.1016/j.tifs.2024. 104643.

[34] N. Quyen, T. Ngan, H. Phong, T. Hien, and L. Dung, "Extraction of kaffir lime (Citrus hystrix DC.) essential oil by steam distillation and evaluation of chemical constituents," in *IOP Conference Series: Materials Science and Engineering*, May 2020, vol. 991, p. 012015, doi: 10.1088/1757-899X/991/1/012015.

[35] B. Guo, C. Liu, L. Grossmann, and J. Weiss, "Pickering emulsion stabilized by hydrolyzed starch: Effect of the molecular weight," *Journal of Colloid and Interface Science*, vol. 612, pp. 525–535, Apr. 2022, doi: 10.1016/j.jcis.2021.12. 185.

[36] R. Liang, Y. Jiang, W. Yokoyama, C. Yang, G. Cao, and F. Zhong, "Preparation of Pickering emulsions with short, medium and long chain triacylglycerols stabilized by starch nanocrystals and their in vitro digestion properties," *RSC Advances*, vol. 6, pp. 99496–99508, Aug. 2016, doi: 10.1016/j.carbpol.2020.116405.

[37] Y. Qin, C. Liu, S. Jiang, L. Xiong, and Q. Sun, "Characterization of starch nanoparticles prepared by nanoprecipitation: Influence of amylose content and starch type," *Industrial Crops and Products*, vol. 87, pp. 182–190, Sep. 2016, doi: 10.1016/j.indcrop.2016.04.038.

[38] X. Song, G. He, H. Ruan, and Q. Chen, "Preparation and properties of octenyl succinic anhydride modified early indica rice starch," *Starch - Stärke*, vol. 58, pp. 109–117, Feb. 2006, doi: 10.1002/star.200500444.

[39] H. Dong, Q. Zhang, J. Gao, L. Chen, and T. Vasanthan, "Comparison of morphology and rheology of starch nanoparticles prepared from pulse and cereal starches by rapid antisolvent nanoprecipitation," *Food Hydrocolloids*, vol. 119, p. 106828, Oct. 2021, doi: 10.1016/ j.foodhyd.2021.106828.

[40] H. Li, Y. Ma, L. Yu, H. Xue, Y. Wang, J. Chen, and S. Zhang, "Construction of octenyl succinic anhydride modified porous starch for improving bioaccessibility of β-carotene in emulsions," *RSC Advances*, vol. 10, pp. 8480–8489, Feb. 2020, doi: 10.1039/C9RA10079B.

[41] U.A. Basilio-Cortés, L. González-Cruz, G. Velazquez, G. Teniente-Martínez, C. A. Gómez-Aldapa, J. Castro-Rosas, and A. Bernardino-Nicanor, "Effect of dual modification on the spectroscopic, calorimetric, viscosimetric and morphological characteristics of corn starch," *Polymers*, vol. 11, p. 333, Feb. 2019, doi: 10.3390/polym11020333.

[42] M. J. dos Santos Alves, P. M. C. Torres de Freitas, A. R. Monteiro, and G. A. Valencia, "Impact of the acidified hydroethanolic solution on the physicochemical properties of starch nanoparticles produced by anti-solvent precipitation," *Starch - Stärke*, vol. 73, p. 2100034, Sep. 2021, doi: 10.1002/star.202100034.

[43] J. M. Fang, P. A. Fowler, C. Sayers, and P. A. Williams, "The chemical modification of a range of starches under aqueous reaction conditions, *Carbohydrate Polymers*, vol. 55, pp. 283–289, Feb. 2004, doi: 10.1016/j.carbpol.2003.10.003.

[44] L. Dai, C. Sun, Y. Wei, L. Mao, and Y. Gao, "Characterization of Pickering emulsion gels stabilized by zein/gum arabic complex colloidal nanoparticles," *Food Hydrocolloids*, vol. 74, pp. 239–248, Jan. 2018, doi: 10.1016/j.foodhyd. 2017.07.040.

[45] X. Liu, H. Luan, Y. Jinglin, S. Wang, S. Wang, and L. Copeland, "A method for characterizing short-range molecular order in amorphous starch," *Carbohydrate Polymers*, vol. 242, p. 116405, Aug. 2020. doi: 10.1016/j.carbpol.2020. 116405.

[46] J. Zhang, C. Ran, X. Jiang, and J. Dou, "Impact of octenyl succinic anhydride (OSA) esterification on microstructure and physicochemical properties of sorghum starch," *LWT*, vol. 152, p. 112320, Dec. 2021, doi: 10.1016/j.lwt.2021.112320.

[47] L. Niedner and G. Kickelbick, "Amphiphilic titania Janus nanoparticles containing ionic groups prepared in oil–water Pickering emulsion," *Nanoscale*, vol. 16, pp. 7396–7408, Feb. 2024, doi: 10.1039/D3NR04907H.

[48] S. Meyer, S. Berrut, T. I. J. Goodenough, V. S. Rajendram, V. J. Pinfield, and M. J. W. Povey, "A comparative study of ultrasound and laser light diffraction techniques for particle size determination in dairy beverages," *Measurement Science and Technology*, vol. 17, p. 289, Jan. 2006, doi: 10.1088/0957-0233/17/2/009.

[49] S. M. Chisenga, T. S. Workneh, G. Bultosa, and B. A. Alimi, "Progress in research and applications of cassava flour and starch: a review," *Journal of Food Science and Technology*, vol. 56, pp. 2799–2813, May 2019, doi: 10.1007/s13197-019-03814-6.

[50] M. Miao, B. Jiang, and T. Zhang, "Effect of pullulanase debranching and recrystallization on structure and digestibility of waxy maize starch," *Carbohydrate Polymers*, vol. 76, pp. 214–221, Mar. 2009, doi: 10.1016/j.carbpol.2008.10.007.

[51] J. Zhi, S. Huang, X. Zhu, H. J. Adra, K. Luo, and Y. R. Kim, "Impact of solvent polarity on the morphology, physicochemical properties, and digestibility of A-type resistant starch particles," *Food Chemistry*, vol. 418, p. 135942, Mar. 2023, doi: 10.1016/j.foodchem.2023.135942.

[52] S. Hedayati, M. Niakousari, and Z. Mohsenpour, "Production of tapioca starch nanoparticles by nanoprecipitation-sonication treatment," *International Journal of Biological Macromolecules*, vol. 143, pp. 136–142, Jan. 2020, doi: 10.1016/j.ijbiomac. 2019.12.003.

[53] S.F. Chin, S.C. Pang, and S.H. Tay, "Size controlled synthesis of starch nanoparticles by a simple nanoprecipitation method," *Carbohydrate Polymers*, vol. 86, pp. 1817–1819, Oct. 2011, doi: 10.1016/j.carbpol.2011.07.012.

[54] W. D. C. Chacon, K. T. dos Santos Lima, G. A. Valencia, and A. C. A. Henao, "Physicochemical properties of potato starch nanoparticles produced by anti-solvent precipitation," *Starch - Stärke*, vol. 73, p. 2000086, Sep. 2021, doi: 10.1002/star.202000086.

[55] S. Huang, C. Chao, J. Yu, L. Copeland, and S. Wang, New insight into starch retrogradation: "The effect of short-range molecular order in gelatinized starch," *Food Hydrocolloids*, vol. 120, p. 106921, Nov. 2021, doi: 10.1016/j.foodhyd. 2021.106921.

[56] B. Zhang, S. Dhital, E. Haque, and M. J. Gidley, "Preparation and characterization of gelatinized granular starches from aqueous ethanol treatments," *Carbohydrate Polymers*, vol. 90, pp. 1587–1594, Nov. 2012, doi: 10.1016/j. carbpol.2012.07.035.

[57] Y. N. Shariffa, A. A. Karim, A. Fazilah, and I.S.M. Zaidul, "Enzymatic hydrolysis of granular native and mildly heat-treated tapioca and sweet potato starches at sub-gelatinization temperature," *Food Hydrocolloids*, vol. 23, no. 2, pp. 434–440, Mar. 2009, doi: 10.1016/ j.foodhyd.2008.03.009.

[58] K. Prompiputtanapon, W. Sorndech, and S. Tongta, "Surface Modification of Tapioca Starch by Using the Chemical and Enzymatic Method," *Starch - Stärke*, vol. 72, no. 3–4, p. 1900133, Dec. 2020, doi: 10.1002/star.201900133.

[59] Z. Harun et al., "Acid hydrolysis and optimization techniques for nanoparticles preparation: Current review," *Applied Biochemistry and Biotechnology*, vol. 194, no. 8, pp. 3779–3801, Apr. 2022, doi: 10.1007/s12010-022-03932-6.

[60] C. Mutungi, L. Passauer, C. Onyango, D. Jaros, and H. Rohm, "Debranched cassava starch crystallinity determination by Raman spectroscopy: Correlation of features in Raman spectra with X-ray diffraction and ^{13}C CP/MAS NMR spectroscopy," *Carbohydrate Polymers*, vol. 87, pp. 598–606, Jan. 2012, doi: 10.1016/ j.carbpol.2011.08.032.

[61] R. Kizil, J. Irudayaraj, and K. Seetharaman, "Characterization of irradiated starches by using FT-Raman and FTIR spectroscopy," *Journal of*

Agricultural and Food Chemistry, vol. 50, pp. 3912–3918, Jun. 2002, doi: 10.1021/jf011652p.

[62] L. Guo, H. Li, L. Lu, F. Zou, H. Tao, and B. Cui, "The role of sequential enzyme treatments on structural and physicochemical properties of cassava starch granules," *Starch - Stärke*, vol. 71, p. 1800258, Feb. 2019, doi: 10.1002/star.201800258.

[63] W. S. Ratnayake and D.S. Jackson, "Starch gelatinization," *Advances in Food and Nutrition Research*, vol. 55, pp. 221–268, Sep. 2008, doi: 10.1016/S1043-4526(08)00405-1.

[64] S. Jiang, L. Dai, Y. Qin, L. Xiong, and Q. Sun, "Preparation and characterization of octenyl succinic anhydride modified taro starch nanoparticles," *PLOS One*, vol. 11, p. e0150043, Feb. 2016, doi: 10.1371/journal.pone.0150043.

[65] Y. Zhu, C. Du, F. Jiang, W. Hu, X. Yu, and S. K. Du, "Pickering emulsions stabilized by starch nanocrystals prepared from various crystalline starches by ultrasonic assisted acetic acid: Stability and delivery of curcumin," *International Journal of Biological Macromolecules*, vol. 267, p. 131217, May 2024. doi: 10.1016/ j.ijbiomac.2024.131217.

[66] H. Yang and J. Irudayaraj, "Characterization of semisolid fats and edible oils by Fourier transform infrared photoacoustic spectroscopy," *Journal of the American Oil Chemists' Society*, vol. 77, pp. 291–295, Mar. 2000, doi: 10.1007/s11746-000-0048-y.

[67] J. No and M. Shin, "Preparation and characteristics of octenyl succinic anhydride-modified partial waxy rice starches and encapsulated paprika pigment powder," *Food Chemistry*, vol. 295, pp. 466–474, Oct. 2019, doi: 10.1016/j.foodchem.2019.05.064.

[68] B. Zhang, J.-Q. Mei, B. Chen, and H.-Q. Chen, "Digestibility, physicochemical and structural properties of octenyl succinic anhydride-modified cassava starches with different degree of substitution," *Food Chemistry*, vol. 229, pp. 136–141, Aug. 2017, doi: 10.1016/j.foodchem.2017.02.061.

[69] M. Lopez-Silva, L. A. Bello-Perez, E. Agama-Acevedo, and J. Alvarez-Ramirez, "Effect of amylose content in morphological, functional and emulsification properties of OSA modified corn starch," *Food Hydrocolloids*, vol. 97, p. 105212, Dec. 2019, doi: 10.1016/j.foodhyd.2019.105212.

[70] F. Kerdmuanglek, T. Chomtong, S. Boonsith, T. Chutimasakul, J. Iemsam-Arng, and S. Thepwatee, "Non-ionic surfactant-assisted controlled release of oxyresveratrol on dendritic fibrous silica for topical applications," *Journal of Colloid and Interface Science*, vol. 646, pp. 342–353, Sep. 2023, doi: 10.1016/ j.jcis.2023.05.050.